

# An attempt to model the influence of gradual transition between cell wall layers on cell wall hygroelastic properties

Ningling Wang · Wangyu Liu · Jiping Lai

Received: 13 September 2013 / Accepted: 12 November 2013 / Published online: 3 December 2013  
© Springer Science+Business Media New York 2013

**Abstract** To better understand the hygroelastic property of wood cell wall, the transition of materials in the area between the S1 and S2 layers is considered in the modeling of cell wall hygroelastic properties. The concentric cylinder model is modified and employed for its compatibility with arbitrary additional layers in different scales. In order to explain the results of the cell wall model, the polymer contribution to the cell wall hygroexpansion is investigated first. Although the amorphous cellulose slightly affects the cell wall hygroexpansion, its influence on the softening of cell wall moduli is not significant. The contributions of hemicellulose and lignin to the hygroexpansion vary as the microfibril angle in the S2 layer changes. The results of the polymer analysis help to explain the effect of the interlayer. Compared to the model without the S1–S2 interlayer, the cell wall swells more in the transverse direction if the transition in the inner S1 layer (S1-part) is considered. For the case of transition in the outer S2 layer (S2-part), the effect reverses. Whilst, in the longitudinal direction, the S1-part amplifies the shrinkage and the S2-part suppresses it. The interlayer affects the cell wall moduli under moisture condition in the same way as under the dry condition. The modeled softening effects can be managed to approach the measurements by adjusting the thickness of the interlayer. We believe that paying more attention to the materials transition between cell wall layers can certainly help us to better understand the cell wall behaviors.

## Introduction

Moisture induced deformation limits the potential of woody resources as structural materials. Tests of the wood materials under moisture conditions have given knowledge of the moisture–mechanical relationship. The moisture related mechanical properties of hemp fiber [1] and beech [2] were studied through tensile tests. Under controlled thermal modifications, the bending response of beech and spruce were also tested [3]. The shrinkage of sugi tree sample was measured under oven-dry conditions [4]. It can be concluded that the cellulose microfibril angle (MFA) [4–7] and chemical composition of wood influence its shrinkage and swelling [8]. Although this deformation of the wood materials can be suppressed through oil treatments without significantly affecting its mechanical properties [9], a better understanding of the hygroelastic behavior is needed for wider applications.

At the microscale, water absorbed between the hydrophilic polymers weakens their original connection, which lowers the elastic moduli of the polymers. The polymer expansion inside the wood cell wall accumulates into the shape change of the wood at the macroscale [10, 11]. Therefore, studying the hygroelastic behaviors of the cell wall is the first step to understand the shrinkage and swelling of wood. The mechanical model plays an important role in these studies [6, 12–14]. Given the properties of the wood polymers, the bottom-up approaches are very suitable for modeling the multi-scale structure of the cell wall. The way we understand the “bottom” of the cell wall, referring to the cell wall ultrastructure and its chemical composition, determines the accuracy of the mechanical model. The following introduction highlights the new perspectives in understanding the cell wall structure and some controversies in polymer properties, which are the primary interests of the present study.

---

N. Wang · W. Liu (✉) · J. Lai  
School of Mechanical and Automotive Engineering, South China  
University of Technology, Guangzhou 510640, China  
e-mail: lucyliuw@163.com

From the view of plant anatomy, the cell wall consists of M, P, S1, S2, and S3 layers at the macroscale. S1, S2, and S3, known as the secondary layers, contribute most to the mechanical properties. Each layer of the secondary wall can be treated as a fiber-reinforced composite material with cellulose microfibrils embedded into the matrix of hemicellulose and lignin. According to the botanical definitions [15], different secondary layers can be characterized by a particular range of MFA. Usually each layer is modeled as a fiber reinforced composite with a specific value of fiber angle. However, a wide range of transition area was observed between the S1 and S2 layers (Observations: [16, 17], measurements: [18]). The MFA and polymer volume fractions are not uniform inside the S1 or S2 layer identified according to the botanical characterization. Therefore, assigning uniform material properties to the S1 or S2 layer actually violates these observations. Rather than ignoring this nonuniformity and obey the botanical definitions, setting up an interlayer between the S1 and S2 layers to represent the transition in the cell wall mechanical model can yield more accurate predictions of cell wall moduli [19]. The transition of MFA and polymer contents between cell wall layers remains as a new concept in the field of cell wall modeling. The influence of the S1–S2 interlayer on the cell wall hygroelastic properties is studied in the present work by considering interlayer in the hygroelastic models.

Hemicellulose and lignin were modeled as hydrophilic in many cases [6, 7, 20]. The normalized elastic modulus of hemicellulose and lignin significantly vary with the relative humidity (RH) [21, 22]. There is no doubt that the matrix of hemicellulose and lignin is the key to understand the moisture-induced softening of the cell wall. Cellulose was treated as completely hydrophobic in several models [7, 20]. However, some researchers modeled the amorphous part of cellulose as accessible to moisture [11, 13, 23]. Salmén [11] hypothesized that 20 % of the volume of the cellulose should absorb water and have the same properties as the hemicellulose. In the longitudinal direction, his model with the amorphous cellulose actually overestimated the softening compared to the measurements. It was concluded that it could be ambiguous whether or not the amorphous cellulose acts as a major softening factor. Rafsanjani et al. [13] concluded that water sorption in the amorphous polymers including the amorphous cellulose makes the cell wall swell and soften. Horvath et al. [23] considered the amorphous cellulose and hemicellulose as accessible to moisture in their model and it was found that the presence of the amorphous cellulose could soften the wood in the longitudinal direction. In summary, it is, however, uncertain whether the amorphous cellulose works as a critical softening contributor to the cell wall.

## Materials and methods

### The modified CC model with the interlayer

The CC model built by Marklund and Varna [6] is valid for modeling an arbitrary number of phases in the CC assembly, which makes it particularly suitable for the present case involving an additional interlayer in the cell wall simplified structure. Each secondary layer was modeled as the concentric cylinder assembled by polymers at the microscale (Fig. 1a). Then the layers were put together to form the entire cell wall at the macroscale. The presence of the interlayer and amorphous cellulose required a four-phase CC model. At the microscale an additional phase of the amorphous cellulose was inserted between the crystalline cellulose and the hemicellulose according to the ultrastructure arrangement depicted by Rafsanjani et al. [13]. At the macroscale, in accordance with our previous study [19], the interlayer was generated between the S1 and S2 layers (Fig. 1b), the transition zone between the S2 and S3 layers was not considered due to its extremely small dimension [18]. It should be noticed that the insertion of the interlayer did not change the thickness of the secondary wall. The interlayer was actually divided from the S1 and S2 layers (Fig. 1b). In order to give space to the interlayer, the S1 and S2 layers need to be narrowed. One part of the interlayer was from the inner S1 (the S1-part) and another part was from the outer S2 (the S2-part). The thickness of the interlayer could be changed by configuring  $t_{int1}$  and  $t_{int2}$ .

### A study in the boundary conditions

In order to discuss the boundary conditions (BC) in the present study, several resultant equations of the CC model are briefly introduced. For a detailed deviation of these equations, the reader is referred to the original CC model [6].

The cell wall hygroexpansion is driven by the softening effect of the amorphous polymers. Therefore the free swelling strain  $\varepsilon_j^H = \beta_j^H \Delta M$  should be subtracted in the strain for the elastic stress–strain relationship

$$\sigma_i = C_{ij} \left( \varepsilon_j - \beta_j^H \Delta M \right) \quad i, j = 1, 2, 3 \quad (1)$$

Here,  $C_{ij}$  is the stiffness matrix in the global coordinate system. The second term in the bracket refers to the swelling strain written as the product of the hygroexpansion coefficient in the  $j$ -direction,  $\beta_j^H$ , and the absorbed moisture weight  $\Delta M$ . 1, 2, 3 refers to the axial, radial, and tangential directions, respectively. Following the standard procedure of an axisymmetric problem under the loading case when no shear stress is developed, each

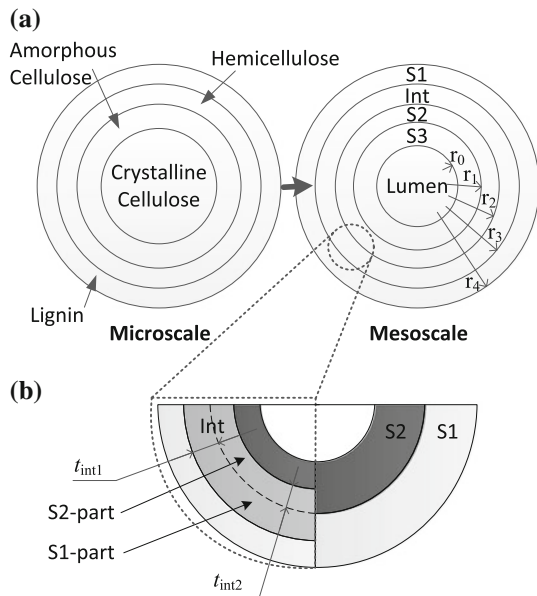


**Fig. 1** **a** The modified concentric cylinder model for the multi-scale modeling of the wood cell wall. The phases of the assemblies at two scales are all labeled. Int refers to the interlayer. The radial coordinates of the interfaces can be related to the volume fractions of the phases. **b** The location of the interlayer.  $t_{int1}$  and  $t_{int2}$  are the thicknesses of the S1-part and S2-part

assembly in the CC model can be solved considering the stress equilibrium equation and the strain–displacement relationship. The derived radial displacement, radial, and axial stresses for the  $k$ th phase can be given by:

$$\begin{bmatrix} u_r^k \\ \sigma_r^k \\ \sigma_\theta^k \\ \sigma_1^k \end{bmatrix} = \begin{bmatrix} r^{\alpha_k} & r^{-\alpha_k} \\ b_k r^{\alpha_k-1} & \gamma_k r^{-\alpha_k-1} \\ f_k r^{\alpha_k-1} & h_k r^{-\alpha_k-1} \end{bmatrix} \begin{bmatrix} A_1^k \\ A_2^k \end{bmatrix} + \epsilon_{10} \begin{bmatrix} \psi_k r \\ \phi_k \\ g_h \end{bmatrix} - \Delta M_k \begin{bmatrix} H_k^* r \\ H_k^r \\ H_k^1 \end{bmatrix} \quad (2)$$

Here,  $r$  and  $\epsilon_{10}$  are the radial coordinate and the axial strain, respectively.  $H_k^*$ ,  $H_k^r$ ,  $H_k^1$ ,  $\alpha_k$ ,  $\psi_k$ ,  $b_k$ ,  $\gamma_k$ ,  $\phi_k$ ,  $f_k$ ,  $h_k$ ,  $g_h$  are all functions of the components of  $C_{ij}$  and  $\beta_i$ . They can be treated as constants once the  $k$ th phase is defined. Detailed forms of these functions can be found in [6]. Then the unknown constants  $A_1^k$ ,  $A_2^k$  and  $\epsilon_{10}$  can be solved by considering the BCs.

- 1) The radial stresses and displacements at the interfaces of adjacent phases should be the same.
- 2) The radial stress at the outer boundary of the assembly should be zero.
- 3) Zero average stress in direction 1.
- 4) Zero radial displacement at the symmetric axis.

BC 1–3 are valid and employed by many models in the cylindrical coordinates. BC 4 is only valid for the situations when the center phase is not empty (filled cell case Fig. 1a). However, the empty center phase is often the case

**Table 1** The center phase BCs for the macroscale calculations

Cases of the center phase	The BCs	Related property constants
Empty	$\sigma_r^1 _{r=r_0} = 0$	–
Filled with resin	$u_r^1 _{r=0} = 0$	Resin properties <sup>a</sup> : $E = 3.0\text{GPa}$ , $\nu = 0.35$ , $\rho = 1.3\text{ g/cm}^3$ $\beta = 0.7$ , $\Delta M = 0.02$ at 80 %RH

<sup>a</sup> The engineering coefficients, density, hygroexpansion coefficient and the moisture weight at 80 % relative humidity of the resin in the original CC model [6] are employed

at the macro-scale (empty cell case). Compared to BC 4, the zero radial stress at the inner boundary seems to be a better BC for the empty center phase (Table 1). The BCs for the inner boundary listed in Table 1 are individually applied in the modified CC model. The cell lumen in the filled cell case needs to be filled with an extra phase of materials, for which resin was used in the original CC model [6]. The present study concerning the filled-cell boundary condition also employs resin as the center phase.

Once  $A_1^k$ ,  $A_2^k$ , and  $\epsilon_{10}$  are solved, the hygroexpansion coefficients can be calculated according to:

$$\beta_1 = \frac{\epsilon_{10}}{\Delta M_{avg}}, \beta_r = \frac{\epsilon_r^{avg}}{\Delta M_{avg}} = \frac{u_r|_{r=r_4} - u_r|_{r=r_0}}{(r_4 - r_0)\Delta M_{avg}} \quad (3)$$

$r_0$  and  $r_4$  are defined in Fig. 1a. The numerator of  $\beta_r$  refers to the radial deformation of the assembly. When the center phase is full,  $r_0$  will be zero. Different from the original CC model, the generalized form of  $\epsilon_r^{avg}$  can serve all kinds of center phase boundary conditions. Since the CC model considers the cell wall as a transversely isotropic material, the radial and tangential hygroexpansion coefficients are the same. The average moisture content of the assembly can be determined as

$$\Delta M_{avg} = \sum_{k=1}^4 \Delta M_k \frac{\rho_k}{\rho_{avg}} V_k, \quad \rho_{avg} = \sum_{k=1}^4 \rho_k V_k \quad (4)$$

The polymer contents and properties

In the present study, the amorphous cellulose, hemicellulose, and lignin all become softened when absorbing water. The measured variations of moisture contents and stiffness of the hemicellulose and lignin under different RH from Cousin were employed (Fig. 2) [22]. Since the crystalline cellulose is hydrophobic, the water absorption in cellulose is mainly contributed by its amorphous part. The amorphous cellulose was modeled as an isotropic material in many cases [23–25]. In the present study, the initial engineering constants of the amorphous cellulose at dry state were assigned with the data from Eichhorn and Young

[26]. The engineering constants and densities of the polymers at dry state were aligned with [6] and listed in Table 2. With the dry state data and measured moduli change under different moisture content (Fig. 2a) [22], the moduli of hemicellulose and lignin can be determined. Then the moduli can be related to RH with the help of the moisture content-RH relation shown in Fig. 2b. Using these data, the cell wall modulus under different RH can be calculated.

A multi-linear regression model was employed by Bergander and Salmén [27] to study the contribution of polymers to the cell wall modulus. Since all three amorphous polymers contribute to the moisture-induced expansion, it is interesting to know the contribution of each amorphous polymer. For this purpose, a multi-linear regression model is also employed. The amorphous cellulose is assumed to have the same softening behavior as the hemicellulose (the same simplification can be found in [11]). Therefore only the hemicellulose and lignin are included in the regression model:

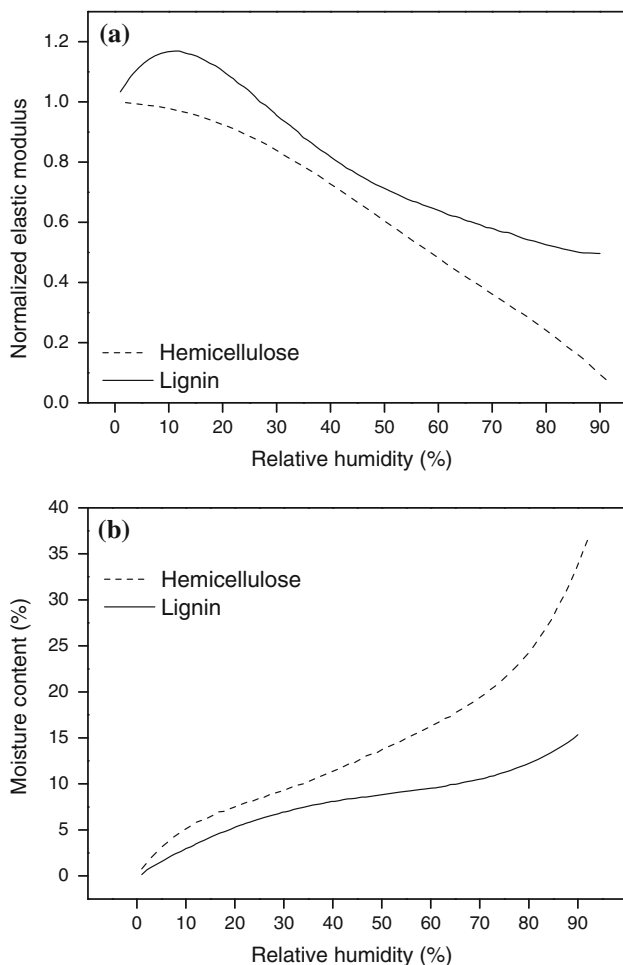


**Fig. 2** The measured variation of **a** stiffness and **b** moisture content for hemicellulose and lignin depending on RH from Cousin [22]

$$y = k_h x_h + k_l x_l + \varepsilon \tag{5}$$

The subscripts *h* and *l* refer to the hemicellulose and lignin, respectively.  $\varepsilon$  is the residual error of the regression model. Only linear terms are kept in the regression model with 95 % confidence level. Variations of the hygroexpansion coefficients of the polymers are achieved by setting up different groups of data based on the literature (Table 2). For a complex multi-scale problem, the statistical tool like the regression model can give a numerical analysis based on the input polymer properties and output cell wall properties.

In the modified CC model, the interlayer will be treated as a homogenized layer just like the other layers. However, the polymer volume fractions  $V_{int}$  and MFA  $\theta_{int}$  of the interlayer will obey the arrangement given by

$$V_{int} = V_{S2}\eta + V_{S1}(1 - \eta) \tag{6}$$

$$\theta_{int} = \theta_{S2}\eta + \theta_{S1}(1 - \eta) \tag{7}$$

The subscripts S1 and S2 indicate the properties of the S1 and S2 layers, respectively.  $\eta$  is the material ratio governing the MFA and polymer volume fractions of the interlayer. The transition is less abrupt near the S2 layer [16, 17, 19]. The interlayer should therefore behave more like the S2. So  $\eta$  is held to be 0.8 in the present study. It is highlighted that the transition of materials in the interlayer includes the chemical composition and the MFA, Eqs. 6 and 7 should be effective simultaneously during the cell wall modeling [19]. Once the material properties of the interlayer is settled, the influence of the thickness of the interlayer on the cell wall hygroelastic properties can be studied by changing  $t_{int1}$  and  $t_{int2}$  (Fig. 1b).

## Results and discussion

### The influences of the boundary conditions

For a clear reference, the interlayer and the amorphous cellulose are not included in the study of different boundary conditions at the center phase. During the modeling in the center phase, the volume fraction of the cell lumen is 36 %. The moisture condition is set to be 80 % RH.

In all cases (Fig. 3), the modeled longitudinal dimension change is relatively small ( $\beta_L < 0.2$ ) within the normal range of S2 MFA for wood (0°–30°) while the moisture-induced expansion in the transverse directions is of considerable magnitude from 0.4 to 0.6, which matches the description in [28]. The crossovers of the hygroexpansion coefficients in different directions all occur in the MFA range from 40° to 50°, which also agrees with the results from literature (modeled results:[6, 12], measurements of *Pinus jeffreyii*: [29]). Similar to the discussion from

**Table 2** Polymer constants used in the present study

Polymers	Crystalline cellulose	Amorphous cellulose		Hemicellulose		Lignin	
Engineering constants at dry state							
$E_1$ (GPa)	150 [6]	5.0 [26]		8.0 [6]		6.0 [6]	
$E_2$ (GPa)	17.5 [6]	5.0 [26]		3.4 [6]		6.0 [6]	
$G_{12}$ (GPa)	4.5 [6]	1.85 [26]		1.2 [6]		2.26 [6]	
$\nu_{12}$	0.1 [6]	0.35 [26]		0.33 [6]		0.33 [6]	
$\nu_{23}$	0.5 [6]	0.35 [26]		0.43 [6]		0.33 [6]	
Polymers	Crystalline cellulose	Amorphous cellulose		Hemicellulose		Lignin	
		A	B	A	B	A	B
Hygroexpansion coefficients							
$\beta_1$	0	0.5	1.368	0	0	0.33	0.351
$\beta_2$	0	0.5	1.368	0.5 [22]	1.368 [34]	0.33	0.351
$\beta_3$	0	0.5	1.368	0.5	1.368	0.33	0.351
Volume fraction							
S1	0.16	0.04		0.15		0.65	
S2	0.392	0.098		0.27		0.24	
S3	0.392	0.098		0.27		0.24	
Densities at dry state (g/cm <sup>3</sup> )	1.55	1.51 [35]		1.49		1.40	

Rafsanjani et al. [5], the small value of S2 MFA generates large anisotropy ratio which reflects in large values of the ratio  $\beta_T/\beta_L$  at small S2 MFAs in Fig. 3. In the longitudinal direction, increasing S2 MFA leads to a larger shrinkage strain [30].

Given the boundary condition of zero radial stress at the inner surface, the cell wall is more drastically softened. However, at small S2 MFAs, the hygroexpansion coefficients of the cell wall in the filled cell case are slightly bigger than those in the empty cell case. For the empty cell case, when the S2 MFA is small, the erect hydrophobic CMF strongly suppresses the radial free expansion of the inner surface in empty cell case [31]. For the filled cell case, the resin in the center phase is modeled with a big hygroexpansion coefficient (0.7), which makes its radial deformation (0.4156  $\mu\text{m}$ ) almost equal to that in the empty cell (0.4154  $\mu\text{m}$ ) at low S2 MFAs. However, the moisture uptake of the resin (0.02) is rather small compared to the cell wall layers (around 0.1) at 80 % RH, which makes the average moisture content of the filled cell smaller than that of the empty cell. The radial hygroexpansion coefficient is calculated by  $\beta_R = \varepsilon_R/\Delta M$ . Therefore, the  $\beta_R$  of the filled cell actually exceeds that of the empty cell at low S2 MFAs. However, the displacements of the inner and outer surfaces are both unconstrained in the empty cell case, which probably increases the uncertainty of the deformation, causing small fluctuations of the hygroexpansion coefficients through the investigated S2 MFA range. The fluctuation may affect the hygroelastic study on the S1–S2

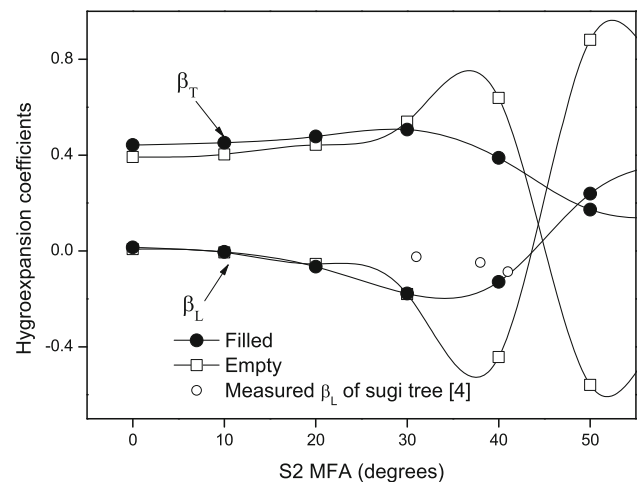


**Fig. 3** The influences of the boundary conditions on the hygroexpansion coefficients. The measurements refer to data of sugi tree [4]

interlayer. Also in the longitudinal direction the curve calculated with the filled cell boundary condition is closer to the measured data of sugi tree (Japanese cedar) [4] than that with the empty cell boundary condition. Therefore, the results given in the following sections were all from models constraining the inner surface.

#### The contribution of the amorphous polymers

The amorphous part of the cellulose significantly lowers the cell wall moduli (Fig. 4a, b). The main reason is that

the presence of amorphous cellulose leads to a decrease in the content of crystalline cellulose which is about 30 times stiffer than the amorphous part [26]. Considering the importance of cellulose microfibrils in determining the cell wall properties [27], the reduction of elastic moduli with the increase of the amorphous ratio can be explained. However, in the longitudinal direction there is no significant variation of the softening magnitudes when the amorphous ratio is varied (Fig. 4a), which can be explained by considering the fact that the amorphous cellulose can be treated as a part of the amorphous matrix covering the crystalline cellulose [11, 32]. And the impact of the matrix on the longitudinal properties is negligible compared to the crystalline cellulose [27]. In the transverse direction, the situation changes (Fig. 4b). The softening magnitude is slightly amplified as the amorphous ratio increases. This effect can be attributed to the bigger contribution of the amorphous matrix to the cell wall transverse properties [11, 27]. Whereas, by introducing the amorphous cellulose, the hygroexpansion coefficients increase in both directions (Fig. 4c). But this increase could almost be negligible at small S2 MFAs (<20°). The longitudinal hygroexpansion coefficients modeled with the amorphous cellulose actually deviate from the measurements at the S2 MFAs around 40°. In summary, under the assumption that the amorphous cellulose has the same softening behaviors as the hemicellulose, the cell wall softening in the transverse direction is more sensitive to the change of amorphous ratio than that in the longitudinal direction. And the influence of the amorphous cellulose on the hygroexpansion should only be considered in the occasion when the S2 MFA exceeds 20°.

The regression coefficients of the hemicellulose and lignin with 95 % confidential intervals are plotted in Fig. 5. The hemicellulose only contributes to the shrinkage in the longitudinal direction (negative coefficients). In the S2 MFA range from 20° to 40°, the hemicellulose has a dominant influence. The positive effect of the lignin becomes pronounced when the angle exceeds 40°. The discrepancies between two polymers are small at S2 MFAs smaller than 20°. In the transverse contribution, the lignin is just as important as the hemicellulose at small S2 MFAs. But the transverse hygroexpansion coefficient becomes more sensitive to the hemicellulose once the angle exceeds 30°. These results are very helpful in the explanation of the behavior of the interlayer in the following section.

The influence of the interlayer

From the view of cell wall ultrastructure, the presence of the interlayer makes the transition between the S1 and S2 less abrupt, which obeys the materials continuity of natural growth. From the results of our previous research, the model with the interlayer between the S1 and S2 can give

more accurate predictions of cell wall elastic modulus than that without the interlayer. In this section, the influence of the interlayer on the cell wall hygroelastic properties is unveiled. The boundary conditions are aligned to those of the filled cell case and data in Group A from Table 2 are employed as hygroexpansion coefficients for the polymers. First, the S1-part and S2-part are independently studied. Then they are combined to show the effect of the interlayer on the softening behavior of the cell wall.

In the transverse direction, the hygroexpansion coefficient of the cell wall with the S2-part is smaller compared to the traditional no-interlayer model, and the differences tend to disappear as the S2 MFA exceeds 30° (Fig. 6). Actually, taking the outer S2 layer as the S2-part of the interlayer causes an increase of lignin content and a decrease of the hemicellulose content in the cell wall.

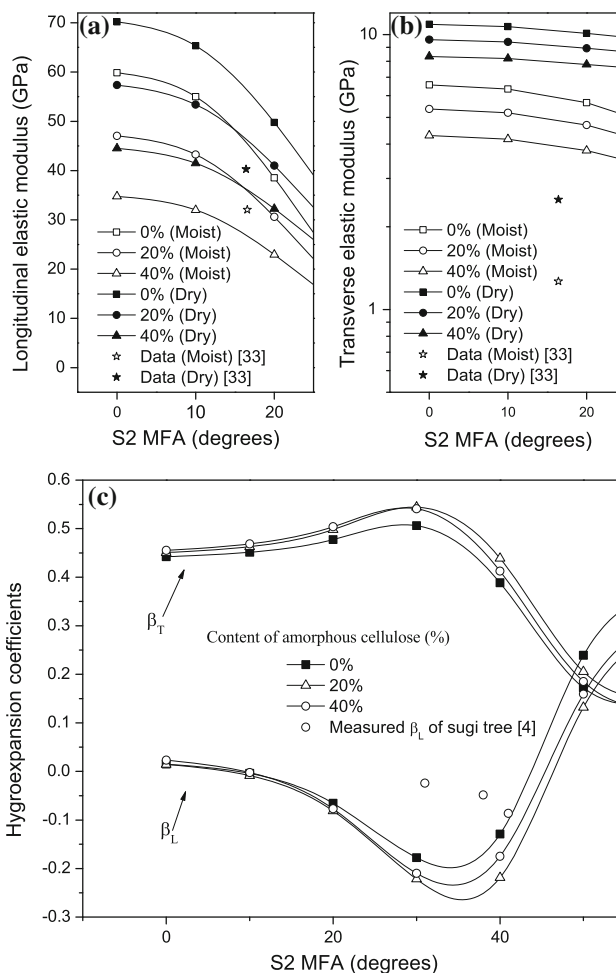


**Fig. 4** Softening in the longitudinal (a) and transverse (b) direction with different contents of the amorphous cellulose. Since the cell wall is modeled as a transversely isotropic material, the transverse direction includes the tangential and radial direction. Measurements refer to data of softwood from [33]. c The influence of the content of the amorphous cellulose on the cell wall hygroexpansion coefficients. The measurements refer to data of sugi tree [4]

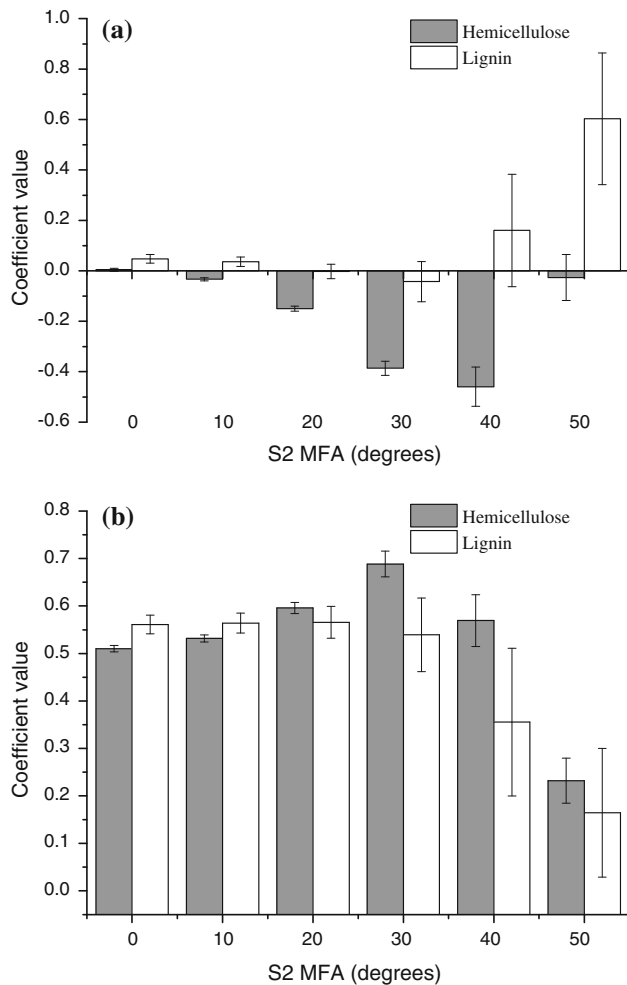


**Fig. 5** The regression coefficients with 95 % confidence intervals from the two-factor linear regression model of the hygroexpansion coefficients in **a** the longitudinal direction and **b** the transverse direction under the investigated S2 MFAs. RH = 80 %

However, before the S2 MFA reaches 30°, both polymers almost equally contribute to the transverse hygroexpansion according to Fig. 5b. So it is hard to explain the results just from the view of polymer contribution. It needs to be reminded that replacing the outer S2 as the S2-part also affects the cell wall modulus (Fig. 7b). This replacement significantly stiffens the cell wall in the transverse direction. Smaller deformations at the cell wall level can be accumulated by the water uptake, which explains the smaller transverse hygroexpansion coefficient before 30°. After the S2 MFA reaches 30°, the influence of the hemicellulose on the transverse hygroexpansion becomes significant. Therefore, the reduction in the content of hemicellulose in the S2-part keeps the transverse hygroelastic coefficients lower than the no-interlayer value. But this effect cannot be maintained at large values of S2 MFA where the effect of the lignin becomes strong (Fig. 5b). Given the fact that more lignin exists in S2-part, the

discrepancies of hygroexpansion coefficients eventually disappear at high S2 MFAs (Fig. 6). Unsurprisingly, the model only with the S1-part gives the reversed results, which can also be explained following the same route.

In the longitudinal direction, the modulus of the cell wall with the S1-part is almost the same as that of the traditional model (Fig. 7a). But the difference between the contributions of hemicellulose and lignin to the cell wall hygroexpansion is significant in the longitudinal direction (Fig. 5a). Replacing the inner S1 layer as the S1-part increases the total content of the hemicellulose and reduces that of the lignin, which keeps the negative values for the longitudinal hygroexpansion coefficient of the cell wall with the S1-part (Fig. 6). As the S2 MFA changes, the discrepancy between the coefficients modeled with and without the S1-part fluctuates according to the variation of the hemicellulose contribution (Fig. 5a). For the cell wall only with the S2-part, the situation varies with the S2 MFA. If the S2 MFA is less than 30°, the cell wall with the S2-part also shrinks more in the longitudinal direction. Once the S2 MFA exceeds 30°, the results are reversed. This phenomenon seems to conflict with the polymer contribution. Since there is less hemicellulose in the S2-part than in the outer S2 layer, it is reasonable to deduce that the longitudinal hygroexpansion coefficient modeled with the S2-part should be bigger at small S2 MFAs where the hemicellulose dominantly devotes to the shrinkage. However, in the similar range of small S2 MFAs, the introduction of the S2-part also significantly reduces the longitudinal cell wall modulus (Fig. 7a). This reduction makes the cell wall much more vulnerable to the shrinkage. Therefore, for the longitudinal hygroexpansion coefficient at low S2 MFAs, the variation of polymer content as we replace the outer S2 with the S2-part devotes to the rise, and the variation of the cell wall longitudinal modulus has a negative effect on the coefficient. It seems that the modulus variation slightly suppresses the effect of the polymer contribution, which yields smaller longitudinal coefficients modeled with the S2-part than the no-interlayer values at small S2 MFAs. Once the S2 MFA exceeds 30°, the difference of the longitudinal modulus between the cell wall with and without the S2-part diminishes (Fig. 7a). Then, the cell wall shrinkage is mainly governed by the polymer contribution according to which less hemicellulose and more lignin in the S2-part bring up the curve. The curve modeled with the S2-part is more close to the central point of the measured longitudinal shrinkage of samples from sugi tree [4], indicating the fact that the materials transition between cell wall layers should be paid more attention in the mechanical models.

Due to the fact that the matrix of hemicellulose and lignin is softened under moist conditions, the rigid cellulose microfibrils become more important in maintaining the

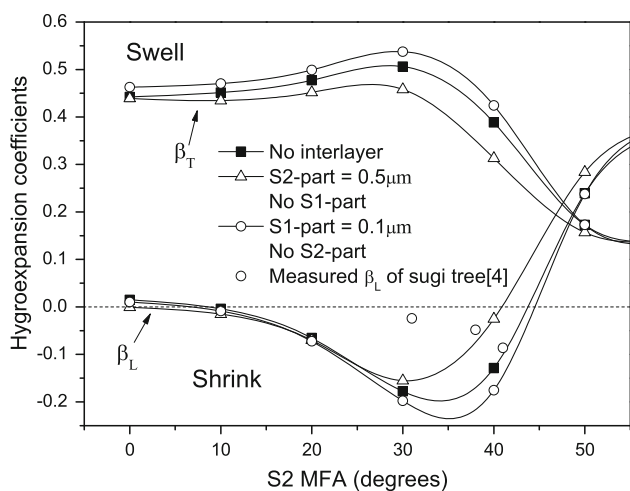


**Fig. 6** The influences of the S1-part and the S2-part on the cell wall hydroexpansion coefficients. RH = 80 %. The measurements refer to data of sugi tree [4]

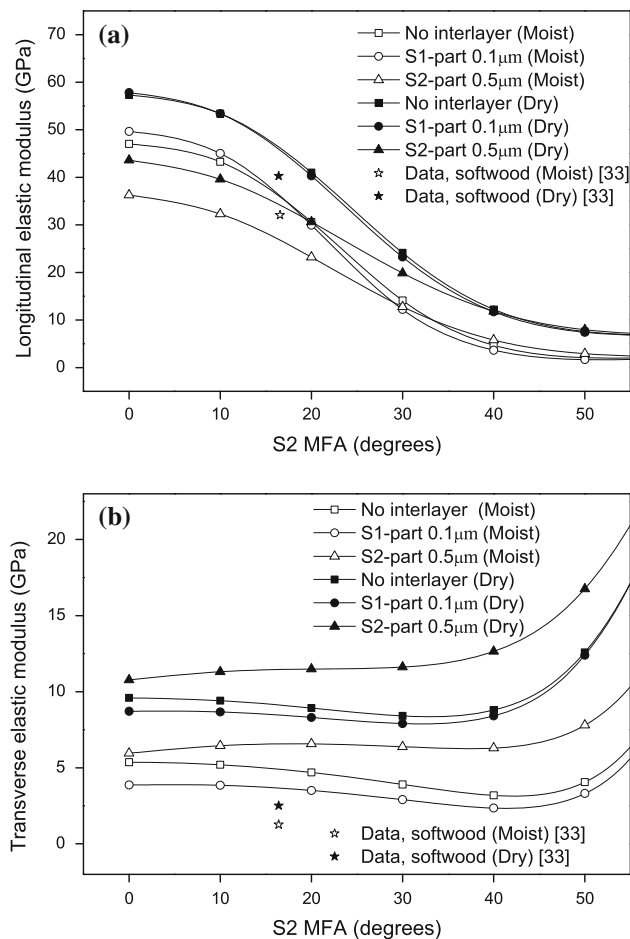


**Fig. 7** The influences of the S1-part and S2-part on the soften behavior of the cell wall in **a** the longitudinal direction and **b** the transverse direction. Measurements refer to data of softwood from [33]

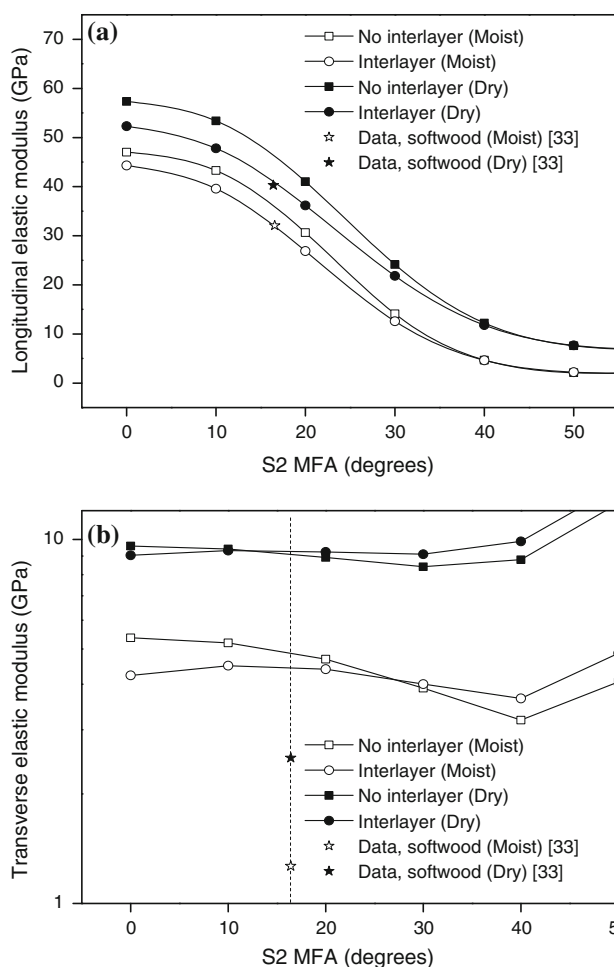


**Fig. 8** The modeled longitudinal **(a)** and transverse **(b)** softening in the cell wall elastic modulus with the interlayer configured as  $t_{int1} = 0.1 \mu\text{m}$  and  $t_{int2} = 0.2 \mu\text{m}$ . Measurements refer to data of softwood from [33]

longitudinal elastic properties. Therefore when the cellulose content is changed by introducing different parts of the interlayer, a bigger variation of cell wall modulus occurs under moist condition (Fig. 7a). This difference is clearly amplified at small S2 MFAs where the cellulose microfibrils are critical to the cell wall elastic properties in the longitudinal direction. Since the matrix dominates the transverse elastic properties of the wood cell wall [27], the softening of matrix brings down all the modeled curves from the dry state (Fig. 7b). But it does not significantly affect the variation between different curves under moist condition.

The present modeled results also show that under wet condition, each part of the interlayer (Fig. 7a, b) exhibits similar effects that were discussed at dry state [19]. The S2-part of the interlayer can lower the longitudinal modulus and increase the transverse modulus, while the S1-part



almost exerts the opposite effects on the cell wall modulus. The effects of both parts get stronger when they become thicker. Considering the effects of the S1-part and S2-part, the modeled softening of elastic modulus can be managed to approach the measurements by adjusting  $t_{int1}$  and  $t_{int2}$ . The configuration of  $t_{int1} = 0.1 \mu\text{m}$  and  $t_{int2} = 0.2 \mu\text{m}$  gives a good agreement between the modeled and measured softening effect in the longitudinal direction (Fig. 8a). Similar to the results from Salmén [11], shifting the data up can give a good match to the modeled ones with the interlayer in the logarithmic scale (Fig. 8b). The interlayer between the S1 and S2 layers clearly has significant influences on the cell wall hygroelastic properties. Ignoring the transition between cell wall layers lowers the accuracy of the hygroelastic models.

## Conclusions

The transition zone between the cell wall layers has a strong influence on the cell wall hygroelastic properties. Substituting the S1-part for the inner S1 layer causes larger transverse shrinkage of the cell wall. The effect reverses as the outer S2 is replaced by the S2-part. The result in the longitudinal direction is not consistent through the whole S2 MFA range. The S1-part and S2-part both amplified the shrinkage at small S2 MFAs, but the S2-part actually suppresses the shrinking as the S2 MFA grows bigger than  $20^\circ$ . For the influence on the cell wall moduli, the behavior of the interlayer under the moisture conditions is the same as that under the dry condition. It is also shown that the measured moisture-induced reduction of cell wall moduli can be predicted by adjusting the thickness of the interlayer.

The boundary conditions for the CC model and the polymer contribution to the cell wall hygroexpansion are also investigated. Applying zero stress at the inner boundary seems to drive the hygroexpansion results of the modified CC model away from the measured data. The amorphous cellulose slightly affects the softening of the cell wall moduli in the transverse direction and has no significant impact on the longitudinal softening. The modeled longitudinal hygroexpansion coefficients with the amorphous cellulose also deviate from the measurements. For the cell wall shrinkage and swelling, the contributions of the hemicellulose and lignin vary with the S2 MFA. In the transverse direction, the hemicellulose and lignin are equally important in the wide range from  $0^\circ$  to  $30^\circ$ . Outside this range, the hemicellulose contributes more. For the contribution to the longitudinal hygroexpansion coefficient of the cell wall, the two polymers are roughly the same until the S2 MFA reaches  $20^\circ$ . The hemicellulose first dominates when the S2 MFA ranges from  $20^\circ$  to  $40^\circ$ , and

then the influence of the lignin becomes pronounced as the S2 MFA exceeds  $40^\circ$ .

**Acknowledgements** The authors gratefully acknowledge the financial support from the National Natural Science Foundation of China (NO. 50975067 & NO. 51375169). The authors wish to acknowledge the precious help from Erik Marklund in the coding of the CC model. Also the helpful comments from the reviewers are deeply appreciated.

## References

1. Placet V, Cisse O, Boubakar ML (2011) Influence of environmental relative humidity on the tensile and rotational behaviour of hemp fibres. *J Mater Sci* 47:3435–3446. doi:10.1007/s10853-011-6191-3
2. Ozyhar T, Hering S, Niemz P (2012) Moisture-dependent elastic and strength anisotropy of European beech wood in tension. *J Mater Sci* 47:6141–6150. doi:10.1007/s10853-012-6534-8
3. Arnold M (2009) Effect of moisture on the bending properties of thermally modified beech and spruce. *J Mater Sci* 45:669–680. doi:10.1007/s10853-009-3984-8
4. Yamamoto H, Sassus F, Ninomiya M, Gril J (2001) A model of anisotropic swelling and shrinking process of wood: Part 2. A simulation of shrinking wood. *Wood Sci Technol* 35:167–181
5. Rafsanjani A, Derome D, Carmeliet J (2012) The role of geometrical disorder on swelling anisotropy of cellular solids. *Mech Mater* 55:49–59
6. Marklund E, Varna J (2009) Modeling the hygroexpansion of aligned wood fiber composites. *Compos Sci Technol* 69:1108–1114
7. Neagu RC, Gamstedt EK (2007) Modelling of effects of ultrastructural morphology on the hygroelastic properties of wood fibres. *J Mater Sci* 42:10254–10274
8. Leonardon M, Altaner CM, Vihermaa L, Jarvis MC (2010) Wood shrinkage: influence of anatomy, cell wall architecture, chemical composition and cambial age. *Eur J Wood Wood Prod* 68:87–94
9. Tomak ED, Viitanen H, Yildiz UC, Hughes M (2010) The combined effects of boron and oil heat treatment on the properties of beech and Scots pine wood. Part 2: Water absorption, compression strength, color changes, and decay resistance. *J Mater Sci* 46:608–615. doi:10.1007/s10853-010-4860-2
10. Yamamoto H, Kojima Y (2002) Properties of cell wall constituents in relation to longitudinal elasticity of wood. Part 1. Formulation of the longitudinal elasticity of an isolated wood f. *Wood Sci Technol* 36:55–74
11. Salmén L (2004) Micromechanical understanding of the cell-wall structure. *C. R. Biol.* 327:873–880
12. Barber NF (1968) A theoretical model of shrinking wood. *Holzforschung* 22:97–103
13. Rafsanjani A, Derome D, Wittel FK, Carmeliet J (2012) Computational up-scaling of anisotropic swelling and mechanical behavior of hierarchical cellular materials. *Compos Sci Technol* 72:744–751
14. Rafsanjani A, Derome D, Carmeliet J (2013) Micromechanics investigation of hygro-elastic behavior of cellular materials with multi-layered cell walls. *Compos Struct* 95:607–611. doi:10.1016/j.compstruct.2012.08.017
15. Wiedenhoeft AC, Miller RB (2005) Structure and function of wood. CRC Press
16. Donaldson L, Xu P (2005) Microfibril orientation across the secondary cell wall of Radiata pine tracheids. *Trees-Struct. Funct.* 19:644–653. doi:10.1007/s00468-005-0428-1
17. Brändström J, Bardage SL, Daniel G, Nilsson T (2003) The structural organisation of the S-1 cell wall layer of Norway spruce tracheids. *Iawa J* 24:27–40

18. Hisashi A, Ohtani J, Fukazawa K (1991) FE-SEM observations on the microfibrillar orientation in the secondary wall of tracheids. *Iawa Bull* 12:431–438
19. Wang N, Liu W, Peng Y (2013) Gradual transition zone between cell wall layers and its influence on wood elastic modulus. *J Mater Sci* 48:5071–5084. doi:[10.1007/s10853-013-7295-8](https://doi.org/10.1007/s10853-013-7295-8)
20. Qing H, Mishnaevsky L (2009) Moisture-related mechanical properties of softwood: 3D micromechanical modeling. *Comp Mater Sci* 46:310–320. doi:[10.1016/j.commatsci.2009.03.008](https://doi.org/10.1016/j.commatsci.2009.03.008)
21. Cousins WJ (1976) Elastic modulus of lignin as related to moisture cont. *Wood Sci Technol* 10:9–17
22. Cousins WJ (1978) Young's modulus of hemicellulose as related to moisture content. *Wood Sci Technol* 12:161–167. doi:[10.1007/bf00372862](https://doi.org/10.1007/bf00372862)
23. Horvath L, Peralta P, Peszlen I, Csoka L, Horvath B, Jakes J (2012) Modeling hygroelastic properties of genetically modified aspen. *Wood Fiber Sci* 44:22–35
24. Hofstetter K, Hellmich C, Eberhardsteiner J (2007) Micromechanical modeling of solid-type and plate-type deformation patterns within softwood materials. A review and an improved approach. *Holzforschung* 61:343–351
25. Katz JL, Spencer P, Wang Y, Misra A, Marangos O, Friis L (2008) On the anisotropic elastic properties of woods. *J Mater Sci* 43:139–145
26. Eichhorn SJ, Young RJ (2001) The Young's modulus of a microcrystalline cellulose. *Cellulose* 8:197–207. doi:[10.1023/a:1013181804540](https://doi.org/10.1023/a:1013181804540)
27. Bergander A, Salmén L (2002) Cell wall properties and their effects on the mechanical properties of fibers. *J Mater Sci* 37:151–156. doi:[10.1023/a:1013115925679](https://doi.org/10.1023/a:1013115925679)
28. Suchsland O, Society FP (2004) *The Swelling and Shrinking of Wood: A Practical Technology Primer*. Forest Products Soc
29. Meylan BA (1968) Cause of high longitudinal shrinkage in wood. *Forest Prod J* 18:75–78
30. Chang S, Quignard F, Di Renzo F, Clair B (2012) Solvent polarity and internal stresses control the swelling behavior of green wood during dehydration in organic solution. *Bioresources* 7:2418–2430
31. Abe K, Yamamoto H (2006) Behavior of the cellulose microfibril in shrinking woods. *J Wood Sci* 52:15–19. doi:[10.1007/s10086-005-0715-x](https://doi.org/10.1007/s10086-005-0715-x)
32. Hofstetter K, Hellmich C, Eberhardsteiner J (2005) Development and experimental validation of a continuum micromechanics model for the elasticity of wood. *Eur J Mech A-solid* 24:1030–1053
33. Kollman FP, Cote W (1968) *Solid Wood. Principles of Wood Science and Technology*, Springer, New York
34. Persson K (2000) *Micromechanical modelling of wood and fibre properties*. Doctor thesis, Department of Mechanics and Materials, Lund University
35. Hatakeyama H, Hatakeyama T (1981) Structural change of amorphous cellulose by water and heattreatment. *Makromol Chem* 182:1655–1668